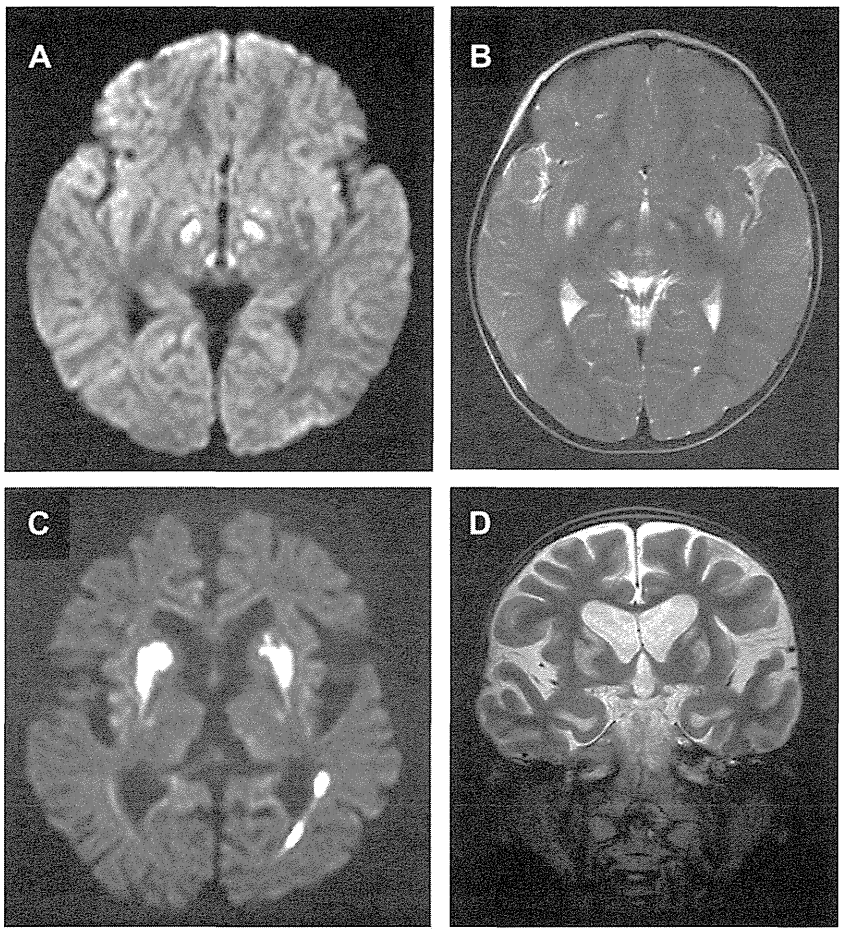

Fig. 1. Diffusion-weighted (A and C) and T2-weighted (B and D) magnetic resonance imaging of the brain in Case 1 at 2 years and 5 months of age (A and B), and in Case 2 at 7 years and 6 months of age (C and D). In Case 1, the bilateral substantia nigra (A), subthalamic nucleus (A and B), red nucleus (A), medial parts of the midbrain (A and B) and putamen (B) show the signal hyperintensity. In Case 2, bilateral striatum reveal hypeintensity (C and D). The left optic radiation is also involved in Case 2 (C) and the global cerebral hemisphere is atrophic (C and D).

2. Case reports

2.1. Case 1

Case 1 is 3-year-old female that was referred to our hospital for an evaluation of failure to thrive and developmental delay at 2 years. She was born to healthy nonconsanguineous Japanese parents. The neonatal period was unremarkable. She held her head upright at 3 months of age, and sat at the 6 months. At the 9 months, she was able to walk independently while holding on to furniture. Her development did not progress thereafter, and she has not walked alone and only speaks using jargon. She was conscious, alert and presented with tachypnea at rest. She displayed facial dysmorphism including frontal bossing, lateral displacement of inner canthi, esotropia, maxillary hypoplasia, slightly upturned nostril, and hypertrichosis dominant on the forehead and extremities. Mild opthalmoplegia and ptosis were noted. She manifested generalized mild hypotonia, truncal ataxia and normal deep tendon reflexes with negative Babinski's signs. Serum lactate was elevated at 35.7 mg/dl. MRI showed signal hyperintensity of the bilateral putamen, subthalamic nucleus, red nucleus and brain stem on T2-weighted images (T2WI) and diffusion-weighted images (DWI) (Fig. 1). The enzyme analysis of the respiratory chain complexes were not performed in this patient.

2.2. Case 2

Case 2 is 8-year-old male on ventilation that was transferred to our hospital for tracheostomy. He was born at term to healthy, nonconsanguineous parents. He had been able to get cruising by 12 months. At 19 months, he presented with neurodevelopmental regression and ataxia. Laboratory investigation revealed elevated cerebrospinal fluid lactate and pyruvate. Brain MRI showed signal hyperintensity of the bilateral basal ganglia, midbrain and medulla oblongata on T2WI. Fibroblast analysis confirmed a decreased amount and activity of complex IV in the respiratory chain complexes

(Fig. 2). He displayed facial dysmorphism including synophrys and micrognathia, hypertrichosis, thoracic deformity and generalized hypotonia and elevated deep tendon reflexes with positive Babinski's signs. MRI showed that the bilateral cerebral hemisphere were globally atrophic and signal hyperintensity of the bilateral optic radiation, putamen, basal ganglia including subthalamic nucleus, and brain stem on T2WI. The left optic radiation, bilateral putamen and globus pallidus also showed high signal intensity on DWI (Fig. 1).

3. Genomic DNA sequencing, RT-PCR and sequencing

Genomic DNA was prepared from white blood cells using the Wizard Genomic DNA purification kit (Promega, Madison, WI, USA). PCR of all exons and exon–intron boundaries of the *SURF1* gene was performed with specific primers using Ex Taq PCR version 1.0 kit (Takara, Shiga, Japan) according to the manufactures instruction (Suppl. Table 1). Total RNA was extracted from leukocytes using Trizol reagent and amplified with the SMART™ mRNA amplification method (Clontech, Mountain View, CA). The amplified mRNA was subjected to reverse transcription with Prime Script reverse transcriptase (Takara, Shiga, Japan) using Oligo (dT) primers. RT-PCR was performed using primers at exons 1 and 9 of the *SURF1* gene, according to the manufacture's instruction (Suppl. Table 1). Patients and families participating in the gene analysis gave written informed consent to the gene analysis, which was approved by the ethical committee of Kanagawa Children's Medical Center.

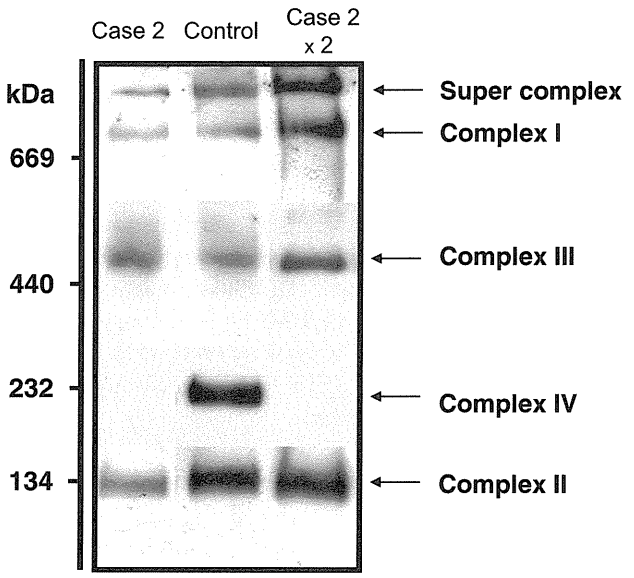

Fig. 2. Analysis of respiratory chain complex amount by blue native polyacrylamide gel electrophoresis in Case 2. Mitochondria isolated from Case 2 and normal control fibroblasts were solubilized in dodecyl maltoside and subjected to BN-PAGE and Western blotting [9]. In x 2 lane, the amount of protein loaded was twice. The amount of fully assembled complex IV was shown to be dramatically decreased in Case 2. The amount of complexes I, II, and III were all comparable to those in the normal control. In vitro enzyme assay [10] also revealed deficiencies of complex IV: the activities of complex I, II, III and IV relative to that of citrate synthase were 137%, 238%, 124% and 12%, respectively.

4. Results

4.1. Case 1

We identified two novel heterozygous mutations: a maternal c.49+1 G>T splice site mutation in intron 1 and a paternal c.752_753del in exon 8. This deletion resulted in a frame shift at amino acid 251(Gln251) causing a stop codon in exon 8 (Fig. 3). The c.49+1 G>T splice site mutation changes the highly conserved G nucleotide at position +1 of the donor splice site (5′ss) in intron 1. We attempted to characterize the splicing outcome of this sequence variation by RT-PCR analysis from patient's blood. Sequence analysis of the RT-PCR reaction detected only the allele with the c.752_753delAG mutation, which implies the presence of a nonsense mediated decay or instability of mRNA from the allele with the c.49+1 G>T splice site mutation.

4.2. Case 2

Sequence analysis of the *SURF1* gene revealed a novel homozygous c.743 C>A, p.Ala248Asp in exon 7. Both parents of this patient were heterozygous for this mutation (Fig. 3). This mutation changes highly conserved Alanine to Aspartate. This mutation was not found in 100 control alleles.

5. Discussion

Molecular elucidation of Leigh syndrome is challenging since many enzymes are involved, such as mitochondrial respiratory chain complexes I, II, III, IV, and V, and components of the pyruvate dehydrogenase complex. Mutation analysis in DNA is more complicated, even after focusing on respiratory complex IV. Mitochondrial-encoded *MTCO3* and nuclear-encoded *COX10*, *COX15*, *SCO2*, and *SURF1*, have been reported as the cause of Leigh syndrome [6,7]. Our two cases presented with mental retardation, failure to thrive, respiratory dysfunction, facial dysmorphism and hypertrichosis. Facial dysmorphism including micrognathia and hypertrichosis especially in the extremities have been reported to be distinctive and characteristic feature of *SURF1* gene mutation [3,4]. Our two cases underscore the importance of *SURF1* analysis in Leigh syndrome with facial dysmorphism and hypertrichosis. However, not all patients with this gene mutation carry these symptoms. Although facial dysmorphism has been also

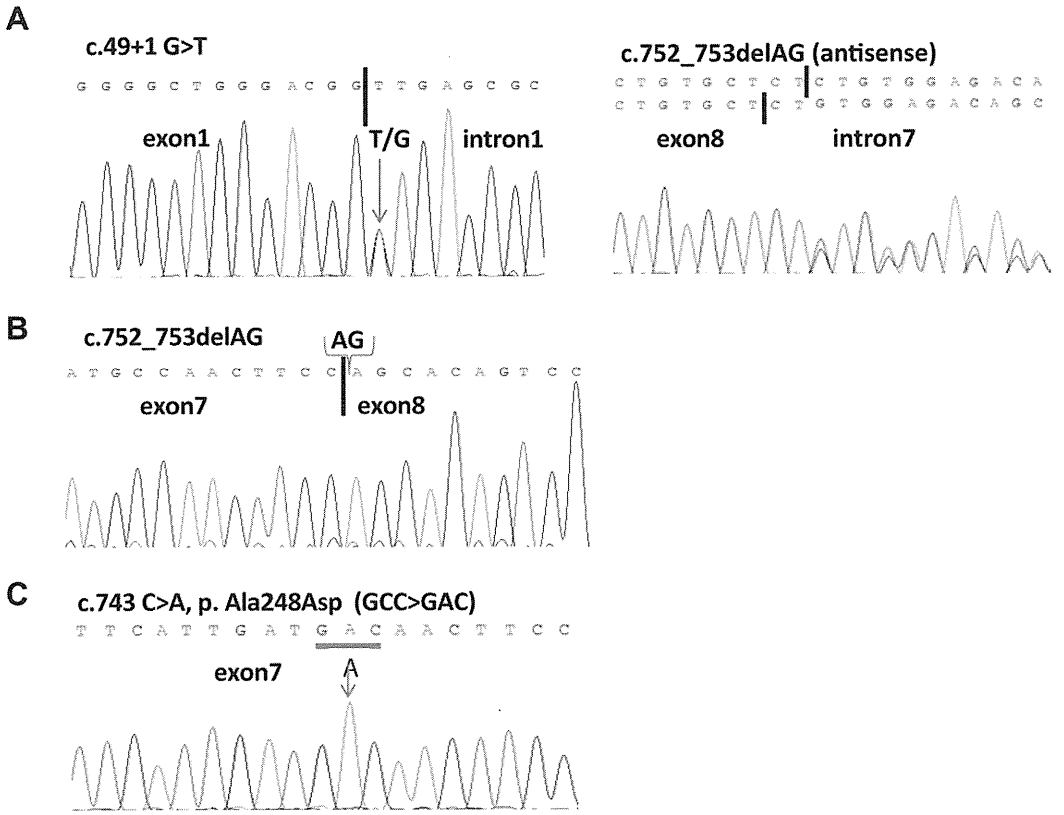

Fig. 3. Analysis of the *SURF1* gene. A chromatogram of the two novel heterozygous mutations; c.49+1 G>T and c.752_753del in Case 1 (A) and homozygous c.743 C>A in Case 2 (C). Panel B shows the chromatogram of cDNA from Case 1. The mutations are shown on the sense strand except for the right panel of A (antisense).

reported in Leigh syndrome with pyruvate dehydrogenase complex, hypertrichosis has not been described [8].

To date, more than 100 patients of Leigh disease with *SURF1* mutations have been reported [6,7]. To our knowledge, this is the first report of a mutation in intron 1, suggesting the need to scan whole exons and exon/intron boundaries.

Common MRI findings of Leigh syndrome are symmetric lesions in the brainstem, basal ganglia, thalamus and spinal cord, Leigh syndrome with *SURF1* mutation have been reported to involved the subthalamic nuclei, medulla, inferior cerebellar peduncles, and substantia nigra [5]. In addition, Case 2 showed signal hyperintensities in bilateral optic radiation on T2WI and DWI, which has not been reported previously in Leigh syndrome with *SURF1* mutations. Since Case 2 had never shown severe hypoxemia, this finding may be significant in patients with *SURF1* mutation or may appear in a progressed stage of disease.

Acknowledgements

This work was supported in part by Grants-in-Aid from Scientific Research from the Ministry of Health, Labor and Welfare of Japan, Health and Labor Science Research Grant of Japan, Yokohama Foundation for Advancement of Medical Science, Takeda Science Foundation, Kanagawa Municipal Hospital Pediatric Research and a grant of the Innovative Cell Biology by Innovative Technology (Cell Innovation Program) from the Ministry of Education, Culture, Sports, Science and Technology, Japan.

Appendix A. Supplementary data

Supplementary data associated with this article can be found, in the online version, at doi:10.1016/j.braindev.2012.02.007.

References

[1] Rahman S, Blok RB, Dahl HH, Danks DM, Kirby DM, Chow CW, et al. Leigh syndrome: clinical features and biochemical and DNA abnormalities. Ann Neurol 1996;39:343–51.
[2] Zhu Z, Yao J, Johns T, Fu K, De Bie I, Macmillan C, et al. SURF1, encoding a factor involved in the biogenesis of cytochrome c oxidase, is mutated in Leigh syndrome. Nat Genet 1998;20:337–43.
[3] Yüksel A, Seven M, Cetincelik U, Yeşil G, Köksal V. Facial dysmorphism in Leigh syndrome with SURF-1 mutation and COX deficiency. Pediatr Neurol 2006;34:486–9.
[4] Ostergaard E, Bradinova I, Ravn SH, Hansen FJ, Simeonov E, Christensen E, et al. Hypertrichosis in patients with SURF1 mutations. Am J Med Genet A 2005;138:384–8.

[5] Rossi A, Biancheri R, Bruno C, Di Rocco M, Calvi A, Pessagno A, et al. Leigh Syndrome with COX deficiency and SURF1 gene mutations: MR imaging findings. AJNR Am J Neuroradiol 2003;24:1188–91.
[6] Shoubridge EA. Cytochrome c oxidase deficiency. Am J Med Genet 2001;106:46–52.
[7] Böhm M, Pronicka E, Karczmarewicz E, Pronicki M, Piekutowska-Abramczuk D, Sykut-Cegielska J, et al. Retrospective, multicentric study of 180 children with cytochrome C oxidase deficiency. Pediatr Res 2006;59:21–6.
[8] Robinson BH, MacMillan H, Petrova-Benedict R, Sherwood WG. Variable clinical presentation in patients with defective E1 component of pyruvate dehydrogenase complex. J Pediatr 1987;111:525–33.
[9] Kirby DM, Salemi R, Sugiana C, Ohtake A, Parry L, Bell KM, et al. NDUFS6 mutations are a novel cause of lethal neonatal mitochondrial complex I deficiency. J Clin Invest 2004;114:v837–845.
[10] Murayama K, Nagasaka H, Tsuruoka T, Omata Y, Horie H, Tregoning S, et al. Intractable secretory diarrhea in a Japanese boy with mitochondrial respiratory chain complex I deficiency. Eur J Pediatr 2009;168:297–302.

Journal of Chromatography B, xxx (2012) xxx–xxx

Contents lists available at SciVerse ScienceDirect

Journal of Chromatography B

journal homepage: www.elsevier.com/locate/chromb

Detection of Δ^4-3-oxo-steroid 5β-reductase deficiency by LC–ESI-MS/MS measurement of urinary bile acids

Akina Muto[a], Hajime Takei[a], Atsushi Unno[a], Tsuyoshi Murai[b], Takao Kurosawa[b], Shoujiro Ogawa[c], Takashi Iida[c], Shigeo Ikegawa[d], Jun Mori[e], Akira Ohtake[f], Takayuki Hoshina[g], Tatsuki Mizuochi[h], Akihiko Kimura[h], Alan F. Hofmann[i], Lee R. Hagey[i], Hiroshi Nittono[a,*]

[a] Junshin Clinic Bile Acid Institute, Haramachi, Meguro-ku, Tokyo 152-0011, Japan
[b] Faculty of Pharmaceutical Sciences, Health Sciences University of Hokkaido, Kanazawa, Ishikari-Tobetsu, Hokkaido 061-0293, Japan
[c] Department of Chemistry, College of Humanities & Sciences, Nihon University, Sakurajousui, Setagaya-ku, Tokyo 156-8550, Japan
[d] Faculty of Pharmaceutical Sciences, Kinki University, Kowakae, Higashi, Osaka 577-8502, Japan
[e] Department of Pediatrics, Kyoto Prefectural University of Medicine Graduate School of Medical Science, Kajii-cho, Kawaramachi Hirokoji, Kamigyo-ku, Kyoto 602-8566, Japan
[f] Department of Pediatrics, School of Medicine, Saitama Medical University, Moroyama, Iruma-gun, Saitama 350-0495, Japan
[g] Department of Pediatrics, Graduate School of Medical Sciences, Kyushu University, Maidashi, Higashi-ku, Fukuoka 812-8582, Japan
[h] Department of Pediatrics and Child Health, Kurume University School of Medicine, Asahi-machi, Kurume-shi, Fukuoka 830-0011, Japan
[i] Department of Medicine, University of California, San Diego, La Jolla, CA 92093-0063, USA

ARTICLE INFO

Article history:
Received 5 January 2012
Accepted 18 May 2012
Available online xxx

Keywords:
Abnormal bile acid
Δ^4-3-Oxo-steroid 5β-reductase deficiency
Inborn errors of bile acid metabolism
Profile
LC–ESI-MS/MS
GC–MS

ABSTRACT

The synthesis of bile salts from cholesterol is a complex biochemical pathway involving at least 16 enzymes. Most inborn errors of bile acid biosynthesis result in excessive formation of intermediates and/or their metabolites that accumulate in blood and are excreted in part in urine. Early detection is important as oral therapy with bile acids results in improvement. In the past, these intermediates in bile acid biosynthesis have been detected in neonatal blood or urine by screening with FAB-MS followed by detailed characterization using GC–MS. Both methods have proved difficult to automate, and currently most laboratories screen candidate samples using LC–MS/MS. Here, we describe a new, simple and sensitive analytical method for the identification and characterization of 39 conjugated and unconjugated bile acids, including Δ^4-3-oxo- and $\Delta^{4,6}$-3-oxo-bile acids (markers for Δ^4-3-oxo-steroid 5β-reductase deficiency), using liquid chromatography-electrospray ionization tandem mass spectrometry (LC–ESI-MS/MS). In this procedure a concentrated, desalted urinary sample (diluted with ethanol) is injected directly into the LC–ESI-MS/MS, operated with ESI and in the negative ion mode; quantification is obtained by selected reaction monitoring (SRM). To evaluate the performance of our new method, we compared it to a validated method using GC–MS, in the analysis of urine from two patients with genetically confirmed Δ^4-3-oxo-steroid 5β-reductase deficiency as well as a third patient with an elevated concentration of abnormal conjugated and unconjugated Δ^4-3-oxo-bile acids. The Δ^4-3-oxo-bile acids concentration recovered in three patients with 5β-reductase deficiency were 48.8, 58.9, and 49.4 μmol/mmol creatinine, respectively by LC–ESI-MS/MS.

1. Introduction

Bile acids are biosynthesized from cholesterol in a process that utilizes multiple partially overlapping enzymatic pathways to make substantial changes to the steroid ring nucleus and side-chain, a process that utilizes a minimum of 16 enzymes [1]. Some of the first inborn errors in these pathways were detected nearly 30 years ago [2,3] by the detection of intermediates in the bile acid biosynthetic pathway. Since that time, inborn errors of bile acid formation involving isolated defects in most of the enzymes in the biosynthetic pathway have been reported [4]. However, such enzymatic defects are extremely rare. The most common genetic defect in bile acid biosynthesis appears to be Δ^4-3-oxo-steroid 5β-reductase deficiency, first described by Setchell et al. [5]. In children with defects in the gene or promoter region of Δ^4-3-oxo-steroid 5β-reductase (gene *AKR1D1*), the urinary bile acid profile contains 7α-hydroxy-3-oxo-4-cholenoic acid (as its glycine *m/z* 444 and taurine *m/z* 494 conjugates), as well as its 12α-dihydroxy-metabolite (again as glycine *m/z* 460 and taurine *m/z* 510 conjugates), as shown in Fig. 1. Chenodeoxycholic acid and cholic acid, the normal primary bile acids in man are nearly undetectable. However,

* Corresponding author at: Junshin Clinic Bile Acid Institute, 2-1-22, Haramachi, Meguro-ku, Tokyo 152-0011, Japan.
E-mail address: bile-res@eco.ocn.ne.jp (H. Nittono).

1570-0232/$ – see front matter © 2012 Published by Elsevier B.V.
http://dx.doi.org/10.1016/j.jchromb.2012.05.023

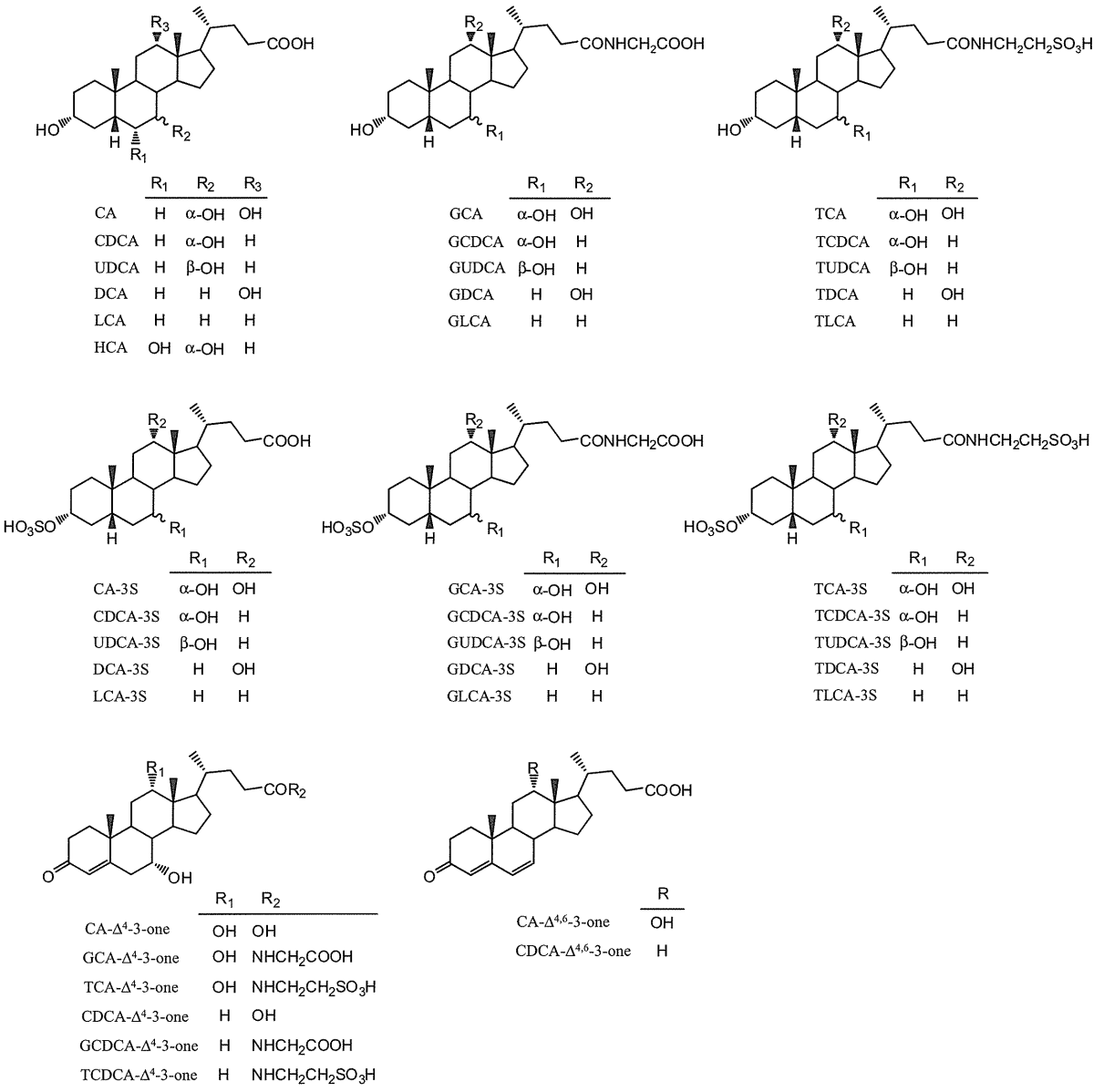

	R_1	R_2	R_3
CA	H	α-OH	OH
CDCA	H	α-OH	H
UDCA	H	β-OH	H
DCA	H	H	OH
LCA	H	H	H
HCA	OH	α-OH	H

	R_1	R_2
GCA	α-OH	OH
GCDCA	α-OH	H
GUDCA	β-OH	H
GDCA	H	OH
GLCA	H	H

	R_1	R_2
TCA	α-OH	OH
TCDCA	α-OH	H
TUDCA	β-OH	H
TDCA	H	OH
TLCA	H	H

	R_1	R_2
CA-3S	α-OH	OH
CDCA-3S	α-OH	H
UDCA-3S	β-OH	H
DCA-3S	H	OH
LCA-3S	H	H

	R_1	R_2
GCA-3S	α-OH	OH
GCDCA-3S	α-OH	H
GUDCA-3S	β-OH	H
GDCA-3S	H	OH
GLCA-3S	H	H

	R_1	R_2
TCA-3S	α-OH	OH
TCDCA-3S	α-OH	H
TUDCA-3S	β-OH	H
TDCA-3S	H	OH
TLCA-3S	H	H

	R_1	R_2
CA-Δ^4-3-one	OH	OH
GCA-Δ^4-3-one	OH	$NHCH_2COOH$
TCA-Δ^4-3-one	OH	$NHCH_2CH_2SO_3H$
CDCA-Δ^4-3-one	H	OH
GCDCA-Δ^4-3-one	H	$NHCH_2COOH$
TCDCA-Δ^4-3-one	H	$NHCH_2CH_2SO_3H$

	R
CA-$\Delta^{4,6}$-3-one	OH
CDCA-$\Delta^{4,6}$-3-one	H

Fig. 1. Chemical structures of unconjugated and conjugated bile acids used in this study.

because gene alterations cannot be found in the majority of patients excreting increased amounts of these urinary Δ^4-3-oxo-bile acids, it was eventually recognized that such abnormal bile acids could also accumulate and be excreted in urine in children with severely damaged liver functions [4]. This turned out to be the case for the first Japanese patient with possible Δ^4-3-oxo-steroid 5β-reductase deficiency [6].

The effects of an accumulation of potentially toxic bile acid intermediates, and the absence of completed bile acid structures, often results in life threatening cholestatic liver disease, and as a result, great emphasis has been placed on early diagnosis and treatment with replacement bile acid therapy. The most non-invasive means of obtaining a preliminary diagnosis is through the analysis of urine for altered bile acids. Most laboratories currently screen candidate samples using LC–ESI-MS/MS [7,8]. Urine samples are examined in the negative mode and searched for the dominant ions present between *m/z* 350 and *m/z* 700 using both the total ion current but also with selected precursor ion scans (parents of 74 for glycine conjugates; parents of 85 for glucuronide conjugates; parents of 97 for sulfate conjugates, and parents of 124 for taurine conjugates). A large number of methods based on LC–MS, with or without CID or multiple reaction monitoring (MRM), have been published, for a summary see Griffiths and Sjövall [9]. Many of these methods produce results that do not always agree with the more comprehensive ion exchange separation followed by GC–MS methods [10]. Recently, Griffiths & Sjövall [11] published a powerful LC–MS/MS method for the complete analysis of oxysterol metabolomes, however, this method is too sensitive and labor intensive for the routine analysis of neonatal urine samples.

Here we describe a new LC–MS/MS method for the analysis of human urinary bile acids. Our aims were to find a method that matched the results obtained by GC–MS methodology, to enable direct analysis of intact bile acid conjugates, to simplify sample preparation, and thus to develop an accurate analytical method that requires a minimum of time and labor. To evaluate the performance of our new method, we compared it to a validated GC–MS method, and then used both methods to analyze the urine from two patients with genetically confirmed Δ^4-3-oxo-steroid 5β-reductase

Please cite this article in press as: A. Muto, et al., J. Chromatogr. B (2012), http://dx.doi.org/10.1016/j.jchromb.2012.05.023

Table 1
LC–ESI-MS/MS date for unconjugated and conjugated bile acids examinated.

Bile acid	RT (min)	Precursor ion (m/z)	Product ion (m/z)	CE (eV)	LOD (pmol/mL)	Correlation coefficient (r^2)
Saturated bile acids						
CA	31.1	407.2	343.2	33	0.50	0.9931
CDCA	34.6	391.3	373.2	32	8.79	0.9903
UDCA	29.5	391.3	373.2	32	14.31	0.9994
DCA	35.2	391.3	345.5	35	1.45	0.9929
LCA	37.9	375.2	357.2	33	21.54	0.9876
HCA	29.2	407.3	389.4	34	1.91	0.9954
GCA	29.5	464.3	74.0	39	0.08	0.9990
GCDCA	32.7	448.3	74.1	42	0.14	0.9995
GUDCA	27.6	448.3	74.1	42	0.19	0.9987
GDCA	33.6	448.3	74.1	42	0.12	0.9999
GLCA	36.0	432.3	74.1	39	0.03	0.9998
TCA	29.4	514.3	124.0	51	1.17	0.9944
TCDCA	32.5	498.3	124.0	51	0.34	0.9985
TUDCA	27.5	498.3	124.0	51	0.14	0.9922
TDCA	33.3	498.3	124.0	51	0.14	0.9933
TLCA	35.7	482.3	124.1	49	0.05	0.9973
CA-3S	24.5	487.3	97.0	46	0.03	0.9960
CDCA-3S	28.4	471.3	97.0	55	1.61	0.9974
UDCA-3S	23.2	471.3	97.0	55	0.30	0.9970
DCA-3S	28.8	471.3	97.0	55	0.64	0.9991
LCA-3S	31.7	455.3	97.0	44	0.01	0.9989
GCA-3S	22.1	271.7	97.0	41	0.05	0.9972
GCDCA-3S	25.5	263.7	97.0	40	0.03	0.9982
GUDCA-3S	20.3	263.7	97.0	40	0.03	0.9987
GDCA-3S	26.1	263.7	97.0	40	0.03	0.9990
GLCA-3S	28.5	255.7	97.0	40	0.37	0.9995
TCA-3S	22.2	296.7	97.0	38	0.04	0.9977
TCDCA-3S	25.4	288.7	97.0	39	0.03	0.9983
TUDCA-3S	20.4	288.7	97.0	39	0.03	0.9967
TDCA-3S	26.1	288.7	97.0	39	0.02	0.9975
TLCA-3S	28.4	280.7	97.0	37	1.13	0.9953
Unsaturated bile acids						
CA-Δ^4-3-one	23.8	403.3	123.1	39	0.09	0.9900
GCA-Δ^4-3-one	22.3	460.3	74.0	37	0.16	0.9992
TCA-Δ^4-3-one	22.4	510.3	124.1	50	0.33	0.9965
CDCA-Δ^4-3-one	29.0	387.3	369.4	27	0.83	0.9880
GCDCA-Δ^4-3-one	27.1	444.3	74.1	35	0.08	0.9980
TCDCA-Δ^4-3-one	27.0	494.3	124.0	44	0.76	0.9946
CA-$\Delta^{4,6}$-3-one	27.6	385.3	341.5	27	0.99	0.9822
CDCA-$\Delta^{4,6}$-3-one	33.2	369.3	325.5	28	0.39	0.9859

RT, retention time; CE, collision energy; LOD, limit of detection (S/N = 5).

deficiency as well as from a third patient with an elevated concentration of abnormal conjugated and unconjugated Δ^4-3-oxo-bile acids.

2. Experimental procedure

2.1. Materials and reagents

Authentic reference bile acids (see Appendix A) used in this study were as follows: cholic acid (CA), glycocholic acid (GCA), taurocholic acid (TCA), chenodeoxycholic acid (CDCA), glycochenodeoxycholic acid (GCDCA), taurochenodeoxycholic acid (TCDCA), ursodeoxycholic acid (UDCA), glycoursodeoxycholic acid (GUDCA), tauroursodeoxycholic acid (TUDCA), lithocholic acid (LCA), glycolithocholic acid (GLCA), taurolithocholic acid (TLCA), deoxycholic acid (DCA), taurodeoxycholic acid (TDCA) and hyocholic acid (HCA) were purchased from Sigma Chemicals (St. Louis, MO, USA). [2,2,4,4-d_4]-CA (d_4-CA, internal standard (IS) for unconjugated bile acids), [2,2,4,4-d_4]-GCA (d_4-GCA, IS for glycine conjugated bile acids), and [2,2,4,4-d_4]-TCA (d_4-TCA, IS for taurine conjugated and double conjugated bile acids) were obtained from CDD Isotopes Inc. (Quebec, Canada). The 3-sulfates for the following bile acids: CA, CDCA, UDCA, DCA, LCA, GCA, GCDCA, GUDCA, GDCA, GLCA, TCA, TCDCA, TUDCA, TDCA, and TLCA were synthesized by a previously reported method [12,13]. Unsaturated bile acids with the Δ^4-3-one configuration in the steroid nucleus for CA, GCA, TCA, CDCA, GCDCA, TCDCA, and for the $\Delta^{4,6}$-3-one for CA, and CDCA were synthesized by a previously reported method [14]. In this paper, we have used semi-trivial nomenclature for the Δ^4-3-one and $\Delta^{4,6}$-3-one derivatives of the common bile acids by using the abbreviation for the saturated compound. Ethanol, methanol, and water were of HPLC grade, ammonium acetate was analytical grade, and all were purchased from Kanto Chemical Co., Inc. (Tokyo, Japan).

2.2. Preparation of standards

Individual stock solutions of bile acids were prepared separately at 10 μmol/mL in ethanol and the stock solutions were stored at −20 °C. These solutions were mixed in equal amounts for the analysis of unknown samples, and five point calibration standard solutions (30, 100, 300, 1000, 3000 pmol/mL) were prepared in 50% ethanol. The calibration standard solutions were stable in analytical glass vials for 4 weeks at 4 °C.

2.3. Urine specimens

Urine samples used for the present analysis were as follows: urines from two patients with 5β-reductase deficiency (as determined by genetic diagnosis, case 2 patient was receiving UDCA); urine from a patient with 5β-reductase deficiency (as determined by urinary bile acids analysis and clinical diagnosis); urine from 9 healthy children (ages 2–3 years); and urine from 5 healthy

Please cite this article in press as: A. Muto, et al., J. Chromatogr. B (2012), http://dx.doi.org/10.1016/j.jchromb.2012.05.023

Table 2
Recovery test of unconjugated and conjugated bile acids examined by LC–ESI-MS/MS.

Bile acids	100 pmol/mL Recovery ($n = 5$, %)			1000 pmol/mL Recovery ($n = 5$, %)		
	Average	(Range)	R.S.D. (%)	Average	(Range)	R.S.D. (%)
Saturated bile acids						
CA	90.6	(87.0–94.8)	3.2	105.6	(86.5–114.7)	10.6
CDCA	91.6	(88.9–97.3)	3.8	107.8	(93.5–120.0)	11.9
UDCA	77.2	(67.0–95.6)	14.1	106.9	(82.8–120.0)	13.8
DCA	91.1	(85.9–95.7)	4.1	106.8	(85.5–117.9)	12.0
LCA	76.5	(70.0–85.4)	8.8	104.7	(96.1–112.5)	5.9
HCA	87.0	(83.2–93.1)	4.2	106.1	(88.0–118.0)	11.1
GCA	104.3	(98.3–106.4)	3.3	91.9	(82.9–108.4)	10.6
GCDCA	101.3	(98.8–103.7)	2.2	93.0	(86.4–109.6)	10.3
GUDCA	100.5	(96.4–104.1)	3.2	89.8	(82.3–109.0)	12.1
GDCA	98.4	(95.0–103.8)	8.2	89.7	(83.3–109.0)	12.0
GLCA	100.0	(95.5–106.2)	4.7	86.7	(83.5–94.0)	5.1
TCA	102.4	(97.4–104.2)	8.9	94.2	(88.9–99.5)	4.6
TCDCA	94.1	(92.2–99.0)	3.0	103.4	(94.8–111.0)	6.0
TUDCA	91.5	(84.0–99.8)	7.2	97.1	(86.4–107.6)	9.5
TDCA	100.9	(89.8–111.4)	7.6	95.2	(89.7–101.6)	5.0
TLCA	97.3	(90.6–100.7)	4.3	99.6	(95.4–105.3)	3.8
CA-3S	101.2	(98.2–003.8)	2.2	97.6	(89.1–104.6)	6.8
CDCA-3S	98.1	(95.5–102.1)	2.7	100.2	(92.7–109.7)	7.2
UDCA-3S	98.3	(94.0–103.2)	4.3	96.2	(89.1–105.8)	6.8
DCA-3S	101.6	(96.9–104.6)	3.2	118.8	(112.8–123.9)	3.5
LCA-3S	98.9	(95.0–102.8)	3.3	98.7	(91.6–103.7)	5.6
GCA-3S	99.3	(96.0–104.3)	3.4	101.2	(94.0–109.8)	6.3
GCDCA-3S	103.2	(98.4–106.7)	3.5	95.3	(88.1–106.2)	7.8
GUDCA-3S	101.1	(97.5–103.5)	2.9	100.8	(88.7–115.0)	9.3
GDCA-3S	103.2	(101.2–104.6)	1.3	106.2	(99.8–108.5)	3.4
GLCA-3S	99.8	(93.6–104.9)	5.6	109.1	(101.0–114.6)	5.2
TCA-3S	100.8	(98.8–103.8)	2.3	102.9	(95.7–112.2)	6.6
TCDCA-3S	98.2	(95.0–99.8)	1.9	103.0	(94.9–110.1)	6.6
TUDCA-3S	99.4	(96.8–102.6)	2.9	94.6	(92.1–98.7)	2.9
TDCA-3S	99.5	(95.4–104.3)	4.1	101.6	(92.3–110.5)	7.6
TLCA-3S	99.5	(96.3–103.0)	2.9	107.4	(99.1–117.9)	6.6
Unsaturated bile acids						
CA-Δ^4-3-one	85.0	(81.8–93.1)	4.4	105.9	(84.2–116.4)	11.9
GCA-Δ^4-3-one	100.1	(96.1–105.6)	3.6	88.2	(79.1–110.1)	14.2
TCA-Δ^4-3-one	94.7	(84.8–103.9)	8.7	94.1	(79.1–105.1)	11.9
CDCA-Δ^4-3-one	92.2	(89.9–94.7)	2.5	104.2	(88.1–112.7)	9.3
GCDCA-Δ^4-3-one	99.3	(96.9–100.9)	1.6	87.7	(81.5–105.4)	11.4
TCDCA-Δ^4-3-one	99.3	(95.1–104.5)	4.0	94.5	(86.5–98.4)	5.1
CA-$\Delta^{4,6}$-3-one	91.3	(87.0–96.0)	4.5	118.0	(96.3–128.3)	11.0
CDCA-$\Delta^{4,6}$-3-one	94.3	(89.4–99.5)	4.1	113.1	(88.7–121.9)	12.4

children (ages 6–8 months). All urine samples were stored at −25 °C until the pretreatment for analysis.

2.4. Sample preparation

For the LC–ESI-MS/MS analysis, 0.05 mL of the urine samples was used for analysis. 0.45 mL of 50% ethanol and IS, 0.5 mL, containing (d_4-CA, d_4-GCA and d_4-TCA 200 pmol/mL in 50% ethanol), was added to the urine. Precipitated solids were moved by filtration through a 0.45 μm millipore filter (Millex®-LG, Billerica, MA, USA). A 10 μL aliquot of the above filtrate was injected directly into the LC–ESI-MS/MS instrument.

2.5. LC–ESI-MS/MS conditions

The LC–ESI-MS/MS system consisted of a TSQ Quantum Discovery Max mass spectrometer (Thermo Fisher Scientific, San Jose, CA, USA) equipped with an ESI probe and Surveyor HPLC system (Thermo Fisher Scientific). A trapping column, Hypersil GOLD column (50 mm × 2.1 mm I.D., 5 μm of particle size; Thermo Fisher Scientific) and a chromatographic separation column, Inertsil Sustain C18 column (150 mm × 2.1 mm I.D., 3 μm particle size; G&L Science, Tokyo, Japan) were employed at 40 °C. A trapping column *via* a column-switching valve was used for the on-line desalting and concentration of urine specimens [15]. After injection of the sample solution, the trapping column was washed with 5 mM ammonium acetate (AA) for 5.5 min at flow rate of 0.1 mL/min, eluted with ethanol, and then transferred into the separation column. A mixture of 5 mM ammonium acetate, ethanol and methanol was used as the eluent, and the separation carried out by linear gradient elution at a flow rate of 0.2 mL/min. The mobile phase composition of ethanol and methanol was gradually changed as follows: ammonium acetate for 3.5 min, ammonium acetate–ethanol (9:1, v/v) for 3.5–4 min, ammonium acetate–ethanol (7:3, v/v) for 4–10 min, ammonium acetate–ethanol–methanol (57:10:33, v/v/v) for 10–16 min, ammonium acetate–ethanol–methanol (2:3:95, v/v/v) for 16–43 min, and then ammonium acetate–ethanol–methanol (2:3:95, v/v/v) for 43–47 min; the column was re-equilibrated for 5 min. Altogether, the total run time was 52 min.

To operate the LC–ESI-MS/MS, the spray voltage and vaporizer temperature were set at 3500 V and 330 °C, respectively. The sheath and auxiliary gas (nitrogen) pressure were set at 50 and 10 arbitrary units, respectively, and the ion transfer capillary temperature was carried out at 330 °C. The collision gas (argon) pressure and the collision energy were kept at 1.3 mm Torr and 27–55 eV, respectively, all in the negative ion mode.

Please cite this article in press as: A. Muto, et al., J. Chromatogr. B (2012), http://dx.doi.org/10.1016/j.jchromb.2012.05.023

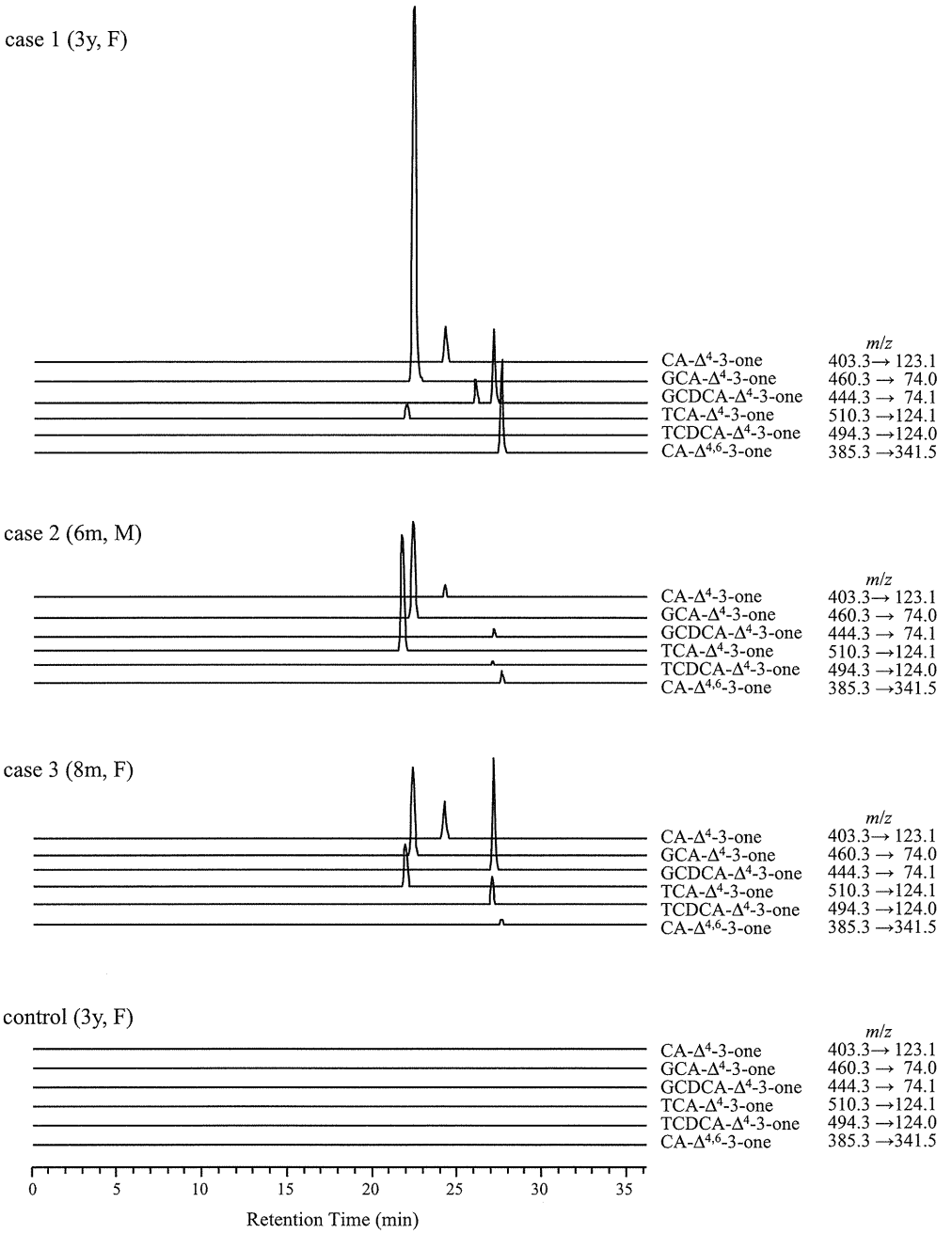

Fig. 2. Selected reaction monitoring chromatograms of urinary bile acids in three patients with 5β-reductase deficiency, as well as healthy control, by LC–ESI-MS/MS.

2.6. Validation of LC–ESI-MS/MS methodology

To characterize the LC–ESI-MS/MS method, we examined specific product ions generated by selecting parent ions and altering the ESI collision energy. Initially, a simultaneous analysis of unconjugated and conjugated bile acids found that a portion of the bile acids were quite sensitive to detection in the positive mode; however, overall, the negative mode was found to be much more appropriate for the measurement of all bile acids as has been reported previously [8]. For the detection of parent ions by ESI, it was possible to select two types of negative ion charges-$[M-H]^-$ for unconjugated bile acids, *N*-acylamidated bile acids and nonamidated bile acid 3-sulfates and $[M-2H]^{2-}$ for the *N*-acylamidated bile acid 3-sulfates [13]. Optimal conditions to conduct the selected reaction monitoring (SRM) were established by the collision-induced dissociation (CID) experiments carried out for each bile acid, and the most suitable collision energy determined by observing the characteristic product ions. The product ions of *N*-acylamidated conjugates were best detected at *m/z* 74.0 (glycine conjugates) and 124.0 (taurine conjugates); sulfated bile acids were best detected at *m/z* 97.0.

2.7. GC–MS analysis

For the GC–MS analysis, an aliquot of 0.5 mL of urine samples before dried and derivatized as a methyl ester-dimethylethyl silyl ether product, as previously described [16]. Ten unconjugated bile acids (CA, CDCA, UDCA, DCA, LCA, HCA, CA-Δ^4-3-one, CDCA-Δ^4-3-one, CA-$\Delta^{4,6}$-3-one and CDCA-$\Delta^{4,6}$-3-one) were used for the GC–MS analysis, which was performed on a Hewlett

Please cite this article in press as: A. Muto, et al., J. Chromatogr. B (2012), http://dx.doi.org/10.1016/j.jchromb.2012.05.023

Table 3
Urinary bile acid profile in three patients with 5β-reductase deficiency and healthy controls by LC–ESI-MS/MS.

	Healthy control (2–3y, $n=9$)	Healthy control (6–8m, $n=5$)	Case 1 (3y)	Case 2[a] (6m)	Case 3 (8m)
Saturated bile acids					
CA	–	–	–	–	–
CDCA	–	–	–	–	–
UDCA	–	–	–	–	–
DCA	–	–	–	–	–
LCA	–	–	–	–	–
HCA	–	–	–	–	–
GCA	–	–	–	–	–
GCDCA	–	–	–	–	–
GUDCA	–	–	–	0.99	–
GDCA	–	–	–	–	–
GLCA	–	–	–	–	–
TCA	–	–	–	–	
TCDCA	–	–	–	–	
TUDCA	–	–	–	–	–
TDCA	–	–	–	–	–
TLCA	–	–	–	–	–
CA-3S	–	–	–	–	–
CDCA-3S	–	–	–	–	–
UDCA-3S	–	–	–	–	–
DCA-3S	–	–	–	–	–
LCA-3S	–	–	–	–	–
GCA-3S	–	–	–	1.51	0.10
GCDCA-3S	0.19 ± 0.14	0.31 ± 0.13	–	–	–
GUDCA-3S	–	–	–	1.64	–
GDCA-3S	0.11 ± 0.16	–	–	–	–
GLCA-3S	0.02 ± 0.04	–	–	–	–
TCA-3S	–	–	–	–	–
TCDCA-3S	0.02 ± 0.03	0.11 ± 0.05	–	–	0.16
TUDCA-3S		–	–	1.10	
TDCA-3S		–	–	–	
TLCA-3S	0.00 ± 0.01	–	–	–	–
Unsaturated bile acids					
CA-Δ^4-3-one	–	–	1.59	0.82	2.58
GCA-Δ^4-3-one	–	–	40.12	22.64	18.23
TCA-Δ^4-3-one	–	–	2.91	33.26	11.85
CDCA-Δ^4-3-one	–	–	–	–	–
GCDCA-Δ^4-3-one	–	–	3.97	1.18	10.38
TCDCA-Δ^4-3-one	–	–	0.17	1.02	6.39
CA-$\Delta^{4,6}$-3-one	–	–	1.10	0.54	0.38
CDCA-$\Delta^{4,6}$-3-one	–	–	–	–	–

Unit: μmol/mmol Cr; Cr, creatinine.
[a] Case 2 patient was receiving UDCA.

Packard 5890 gas chromatograph (Agilent, Santa Clara CA, USA) and Hewlett Packard 5973 mass selective detector instrument (Agilent, Santa Clara CA, USA). A fused-silica capillary column bonded with methylsilicon, DB5MS (30 m × 0.25 mm I.D., 0.25 μm film thickness; Agilent) was used to separate the derivatized bile acids. A carrier gas (helium) of flow rate was 1.4 mL/min. was used, and the column temperature was held at 170 °C for 2 min and then ramped at 10 °C/min until 230 °C ramped again at 3 °C/min. up to 310 °C. Mass spectra were recorded at 70 eV for the ionization energy and at 250 °C for the ion source temperature.

2.8. Method validation

2.8.1. Recoveries of bile acids and ISs during pretreatment

The recoveries of bile acids were calculated from the peak area ratios of unconjugated bile acids/d_4-CA, glycine conjugated bile acids/d_4-GCA, and taurine conjugated and double conjugated bile acids/d_4-TCA, respectively, in sample A and B as described below. The recoveries of ISs were calculated from the peak area ratios of d_4-CA/CA, d_4-GCA/GCA, and d_4-TCA/TCA in sample A and B as described below.

Sample A: the blank urine (0.05 mL) spiked with 39 reference bile acids (100 pmol) was pretreated. After addition of ISs (100 pmol each) to this pretreated urine, the resulting sample was subjected to LC–ESI-MS/MS.

Sample B: the blank urine (0.05 mL) spiked with 39 reference bile acids (1000 pmol) was pretreated. After addition of ISs (100 pmol each) to this pretreated urine, the resulting sample was subjected to LC–ESI-MS/MS.

2.8.2. Reproducibility

The reproducibility was assessed by determining two urine samples at different concentration levels ($n=5$ for each sample) and determined as the relative standard deviation (R.S.D.%).

2.8.3. Assay accuracy (analytical recovery)

50% ethanol (0.45 mL) was added to the urine (the spiked concentrations of bile acids were 100 and 1000 pmol, respectively). After the addition of ISs (100 pmol each), each of the resulting samples were pretreated and analyzed by LC–MS/MS. The assay accuracy (analytical recovery) of bile acids was defined as $F/(F_0+A)\times 100\%$, where F is the concentration of bile acids in the spiked sample, F_0 is the concentration of bile acids in the unspiked sample and A is the spiked concentration.

Please cite this article in press as: A. Muto, et al., J. Chromatogr. B (2012), http://dx.doi.org/10.1016/j.jchromb.2012.05.023

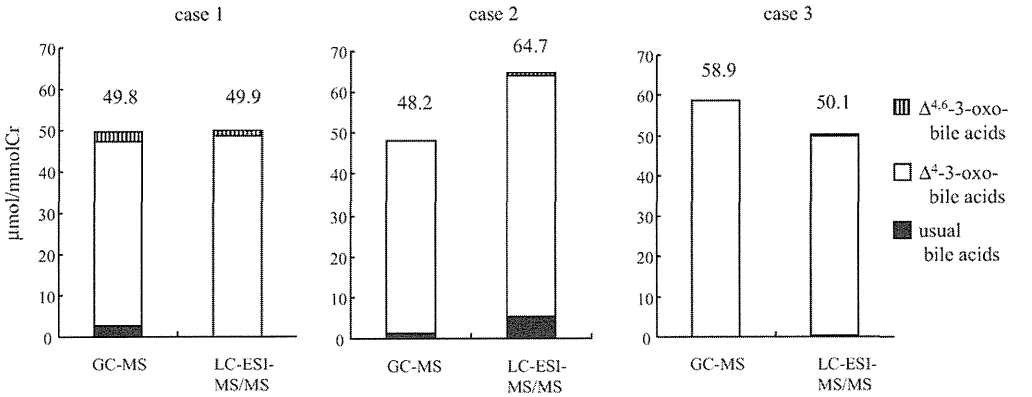

Fig. 3. Comparison of urinary bile acids levels by GC/MS and LC–ESI-MS/MS. Levels shown by GC/MS are the concentration of total bile acids following deconjugation by enzymatic hydrolysis. The results using LC–ESI-MS/MS are the concentration of total unconjugated bile acids combined with their glycine, taurine, and unconjugated bile acid sulfates as well as the *N*-acylamidates of the bile acid sulfates.

3. Results

Fig. 1 shows the chemical structures of the 39 variants of unconjugated and conjugated C_{24} bile acids examined in this study, which include the unconjugated bile acids, *N*-acylamidate conjugates with glycine or taurine at C-24 in the side chain, as well as the C-3 sulfated bile acids in unconjugated and *N*-acylamidated forms. For the initial LC–ESI-MS/MS analysis, we examined the optimum conditions for generating specific product ions arising from the respective parent ions (protonated molecule $[M+H]^+$ or deprotonated molecule $[M-H]^-$) in both the positive and negative ion charge modes. Most of the bile acids showed a high sensitivity and selectivity in the negative mode. Tube lens offset voltage and collision energy of each bile acid, and their conjugates under negative-ion ESI-MS/MS were optimized by directly injecting the standard solution. The most abundant transitions that could be used for monitoring ion are listed in Table 1. The chromatographic conditions, especially the composition of mobile phase, were optimized through several trials. When using an Inertsil Sustain C18 column and a linear gradient elution of ammonium acetate for 3.5 min, ammonium acetate–ethanol (9:1, v/v) for 3.5–4 min, ammonium acetate–ethanol (7:3, v/v) for 4–10 min, ammonium acetate–ethanol–methanol (57:10:33, v/v/v) for 10–16 min, ammonium acetate–ethanol–methanol (2:3:95, v/v/v) for 16–43 min, and then ammonium acetate–ethanol–methanol (2:3:95, v/v/v) for 43–47 min at a flow rate of 0.2 mL/min, satisfactory separation of each bile acid was achieved, and the chromatographic run time was 52 min; retention times and transitions used in SRM for bile acids are given in Table 1. Calibration graphs were then constructed by plotting the peak-area ratio of each bile acid to those of [2,2,4,4-d_4]-CA (IS for unconjugated bile acids), [2,2,4,4-d_4]-GCA (IS for glycine conjugated bile acids), and [2,2,4,4-d_4]-TCA (IS for taurine conjugated and double conjugated bile acids) *versus* the weights of the bile acid. The response was linear with correlation coefficient (r^2) of 0.9822–0.9999 within the range of 30–3000 pmol/mL. The assay reproducibility was examined by 5 repetitive measurement of healthy volunteer's, which contained different concentrations of bile acid. The assay of R.S.D for all the bile acids was less than 14.2%. The assay accuracy was evaluated as the analytical recovery. As shown in Table 2, satisfactory recovery rates ranging from 76.5 to 118.8% were obtained. These data indicate that the present method is highly reproducible and accurate.

Having validated the method for LC–ESI-MS/MS, we then examined the urinary bile acid profiles in a control patient, and in three patients with 5β-reductase deficiency. The results are shown in Fig. 2, in which the abnormal Δ^4-3-oxo bile acids stand out prominently in the three 5β-reductase deficient patients (48.8 μmol/mmol creatinine (Cr), case 1; 58.9 μmol/mmol Cr, case 2; and 49.4 μmol/mmol Cr, case 3), and are completely absent in the normal control. The results of a quantitative determination of total urinary bile acids for two controls and the three 5β-reductase patients are shown in Table 3.

We then analyzed the urines from the three 5β-reductase patients using a validated GC–MS method, and compared the GC–MS results to the data obtained using our LC–ESI-MS/MS methodology. As shown in Fig. 3, both methods gave near identical results, as both the GC–MS and LC–ESI-MS/MS could detect Δ^4-3-oxo and $\Delta^{4,6}$-3-oxo bile acids in these urine samples in a similar proportion. In Fig. 3, the total bile acid concentration recovered in cases 1–3 was 49.8, 48.2, and 58.9 μmol/mmol Cr (respectively) by GC–MS, and 49.9, 64.7, and 50.1 μmol/mmol Cr (respectively) by LC–ESI-MS/MS. Values for urine samples from control subjects done under identical conditions yielded less than 1% Δ^4-3-oxo and $\Delta^{4,6}$-3-oxo bile acids (data not shown).

4. Discussion

The method reported describes a time and labor saving LC–ESI-MS/MS method for human urine that requires only a quick dilution step with alcohol, filtration through a standard 0.45 μm millipore filter, and direct injection into the instrument. In comparison with previously published methods for FAB-MS [17] and GC–MS [18,19], our method is able to separate and identify 39 conjugated and unconjugated bile acids found in urine. In addition, whereas other LC–ESI-MS/MS methods produce results that are often not in accordance with validated GC–MS methods, results obtained with our methodology agree quite well with those obtained by GC–MS. A clear advantage of our method over GC–MS is its ability to detect and quantify the bile acid conjugates and distinguish them from unconjugated bile acids. Thus, our method shows that the Δ^4-3-one bile acids were present as taurine and glycine conjugates. In contrast, the GC–MS method requires a prior enzymatic deconjugation step and thus does not provide such information.

The life-threatening severity of inborn errors of bile acids metabolism, and their need for early detection, has led to a proliferation of non-invasive screening methods. In patients either with confirmed 5β-reductase deficiency, or with severe liver disease, the output of normal bile acids is suppressed and bile acid precursors appear in the urine. Current treatment protocols call for the oral administration of primary bile acids in patients with inborn errors of bile acid biosynthesis, and following the response to treatment by monitoring tests of liver injury. Our quantitative method should

Please cite this article in press as: A. Muto, et al., J. Chromatogr. B (2012), http://dx.doi.org/10.1016/j.jchromb.2012.05.023

enable a real-time monitoring of the effects of the course of treatment, by following the gradual reduction and disappearance of bile acid precursors from the urine.

Appendix A.

Abbreviations and the corresponding trivial names of unconjugated, *N*-acylamidated (with glycine or taurine), and sulfated bile acids used in this study.

CA	Cholic acid
CDCA	Chenodeoxycholic acid
UDCA	Ursodeoxycholic acid
DCA	Deoxycholic acid
LCA	Lithocholic acid
HCA	Hyocholic acid
GCA	Glycocholic acid
GCDCA	Glycochenodeoxycholic acid
GUDCA	Glycoursodeoxycholic acid
GDCA	Glycodeoxycholic acid
GLCA	Glycolithocholic acid
TCA	Taurocholic acid
TCDCA	Taurochenodeoxycholic acid
TUDCA	Tauroursodeoxycholic acid
TDCA	Taurodeoxycholic acid
TLCA	Taurolithocholic acid
CA-3S	Cholic acid 3-sulfate
CDCA-3S	Chenodeoxycholic acid 3-sulfate
UDCA-3S	Ursodeoxycholic acid 3-sulfate
DCA-3S	Deoxycholic acid 3-sulfate
LCA-3S	Lithocholic acid 3-sulfate
GCA-3S	Glycocholic acid 3-sulfate
GCDCA-3S	Glycochenodeoxycholic acid 3-sulfate
GUDCA-3S	Glycoursodeoxycholic acid 3-sulfate
GDCA-3S	Glycodeoxycholic acid 3-sulfate
GLCA-3S	Glycolithocholic acid 3-sulfate
TCA-3S	Taurocholic acid 3-sulfate
TCDCA-3S	Taurochenodeoxycholic acid 3-sulfate
TUDCA-3S	Tauroursodeoxycholic acid 3-sulfate
TDCA-3S	Taurodeoxycholic acid 3-sulfate
TLCA-3S	Taurolithocholic acid 3 sulfate
CA-Δ^4-3-one	7α,12α-Dihydroxy-3-oxo-4-cholenoic acid
GCA-Δ^4-3-one	7α,12α-Dihydroxy-3-oxo-4-cholen-24-oic acid *N*-(carboxymethyl)amide
TCA-Δ^4-3-one	7α,12α-Dihydroxy-3-oxo-4-cholen-24-oic acid *N*-(2-sulfoethyl)amide
CDCA-Δ^4-3-one	7α-Hydroxy-3-oxo-4-cholen-24-oic acid
GCDCA-Δ^4-3-one	7α-Hydroxy-3-oxo-4-cholen-24-oic acid *N*-(carboxymethyl)amide
TCDCA-Δ^4-3-one	7α-Hydroxy-3-oxo-4-cholen-24-oic acid *N*-(2-sulfoethyl)amide
CA-$\Delta^{4,6}$-3-one	12α-Hydroxy-3-oxo-4,6-choladien-24-oic acid
CDCA-$\Delta^{4,6}$-3-one	3-Oxo-4,6-choladien-24-oic acid

References

[1] D.W. Russell, J. Lipid Res. 50 (2009) S120.
[2] H. Eyssen, G. Parmentier, F. Compernolle, J. Boon, E. Eggermont, Biochim. Biophys. Acta 273 (1972) 212.
[3] R.F. Hanson, J.N. Isenberg, G.C. Williams, D. Hachey, P. Szczepanik, P.D. Klein, H.L. Sharp, J. Clin. Invest. 56 (1975) 577.
[4] P.T. Clayton, J. Inherit. Metab. Dis. 34 (2011) 593.
[5] K.D. Setchell, F.J. Suchy, M.B. Welsh, L. Zimmer-Nechemias, J. Heubi, W.F. Balistreri, J. Clin. Invest. 82 (1988) 2148.
[6] A. Kimura, K.H. Kondo, K.I. Okuda, S. Higashi, M. Suzuki, T. Kurosawa, M. Tohma, T. Inoue, A. Nishiyori, M. Yoshino, H. Kato, T. Setoguchi, Eur. J. Pediatr. 157 (1998) 386.
[7] K.A. Mills, I. Mushtaq, A.W. Johnson, P.D. Whitfield, P.T. Clayton, Pediatr. Res. 43 (1998) 361.
[8] I.M. Yousef, S. Perwaiz, T. Lamireau, B. Tuchweber, Med. Sci. Monit. 9 (2003) MT21.
[9] W.J. Griffiths, J. Sjövall, J. Lipid Res. 51 (2010) 23.
[10] J. Sjövall, W.J. Griffiths, K.D. Setchell, N. Mano, J. Goto, in: H.L. Makin, D.B. Gower (Eds.), Steroid Analysis, Springer, 2010, p. 837.
[11] W.J. Griffiths, J. Sjövall, Biochem. Biophys. Res. Commun. 396 (2010) 80.
[12] J. Goto, H. Kato, F. Hasegawa, T. Nambara, Chem. Pharm. Bull. (Tokyo) 27 (1979) 1402.
[13] T. Goto, K.T. Myint, K. Sato, O. Wada, G. Kakiyama, T. Iida, T. Hishinuma, N. Mano, J. Goto, J. Chromatogr. B 846 (2007) 69.
[14] I. Björkhem, H. Danielsson, C. Issidorides, A. Kallner, Acta Chem. Scand. 19 (1965) 2151.
[15] N. Kishi, N. Mano, N. Asakawa, Anal. Sci. 17 (2001) 709.
[16] M. Suzuki, T. Murai, T. Yoshimura, A. Kimura, T. Kurosawa, M. Tohma, J. Chromatogr. B 693 (1997) 11.
[17] F.J. Suchy, R.J. Sokol, W.F. Balistereri (Eds.), Liver Disease in Children, Cambridge University Press, New York, 2007, p. 736.
[18] A. Unno, H. Nittono, H. Takei, T. Tawa, A. Tokita, Y. Yamashiro, M. Matsumoto, A. Kimura, T. Murai, T. Kurosawa, M. Tohma, Jpn. J. Pediatr. Gastroenterol. Hepatol. Nutr. 14 (2000) 25 (in Japanese).
[19] H. Nittono, H. Takei, A. Unno, A. Kimura, T. Shimizu, T. Kurosawa, M. Tohma, M. Une, Pediatr. Int. 51 (2009) 535.

Please cite this article in press as: A. Muto, et al., J. Chromatogr. B (2012), http://dx.doi.org/10.1016/j.jchromb.2012.05.023

J Inherit Metab Dis
DOI 10.1007/s10545-012-9514-x

ORIGINAL ARTICLE

Sustained high plasma mannose less sensitive to fluctuating blood glucose in glycogen storage disease type Ia children

Hironori Nagasaka · Tohru Yorifuji · Robert H. J. Bandsma · Tomozumi Takatani · Hisaki Asano · Hiroshi Mochizuki · Mayuko Takuwa · Hirokazu Tsukahara · Ayano Inui · Tomoyuki Tsunoda · Haruki Komatsu · Eitaro Hiejima · Tomoo Fujisawa · Ken-ichi Hirano · Takashi Miida · Akira Ohtake · Tadao Taguchi · Ichitomo Miwa

Received: 26 December 2011 / Revised: 3 June 2012 / Accepted: 26 June 2012

Abstract Plasma mannose is suggested to be largely generated from liver glycogen-oriented glucose-6-phosphate. This study examined plasma mannose in glycogen storage disease type Ia (GSD Ia) lacking conversion of glucose-6-phosphate to glucose in the liver. We initially examined fasting—and postprandial 2 h—plasma mannose and other blood carbohydrates and lipids for seven GSD Ia children receiving dietary interventions using cornstarch and six healthy age-matched children. Next, one-day successive intra-individual parameter changes were examined for six affected and two control children. Although there were no significant differences in fasting—and postprandial 2 h—glucose and insulin levels, the mannose level of the affected group was invariably much higher than that of the control group ($p<0.001$): the fasting

Communicated by: Alberto B. Burlina

H. Nagasaka (✉) · M. Takuwa
Department of Pediatrics, Takarazuka City Hospital,
Takarazuka 665-0827, Japan
e-mail: nagasa-hirono@k2.dion.ne.jp

T. Yorifuji
Department of Pediatric Endocrinology and Metabolism,
Children's Medical Center, Osaka City General Hospital,
2-13-22 Miyakojima-hondori, Miyakojima-ku,
Osaka 534-0021, Japan

R. H. J. Bandsma
Department of Pediatrics, Center for Liver, Digestive and
Metabolic Diseases, University Medical Center Groningen,
Groningen, Hanzeplein 1,
9700 RB, The Netherlands

T. Takatani
Department of Pediatrics,
Chiba University Graduate School of Medicine,
Chiba 260-8670, Japan

H. Asano · T. Taguchi · I. Miwa
Department of Pathobiochemistry, Faculty of Pharmacy,
Meijo University,
Nagoya 468-8503, Japan

H. Mochizuki
Division of Endocrinology and Metabolism,
Saitama Children's Medical Center,
Saitama 339-8551, Japan

H. Tsukahara
Department of Pediatrics,
Okayama University Graduate School of Medicine,
Okayama 700-8558, Japan

A. Inui · T. Tsunoda · H. Komatsu · E. Hiejima · T. Fujisawa
Department of Pediatrics, Saiseikai Yokohama Tobu Hospital,
Yokohama 230-0012, Japan

K.-i. Hirano
Department of Cardiovascular Medicine,
Osaka University Graduate School of Medicine,
Osaka 565-0871, Japan

T. Miida
Department of Clinical Laboratory Medicine,
Juntendo University School of Medicine,
Tokyo 113-8421, Japan

A. Ohtake
Department of Pediatrics, Faculty of Medicine,
Saitama Medical University,
Iruma-Gun, Saitama 350-0495, Japan

Published online: 13 September 2012

level of the affected group was about two-fold that of the control group; the postprandial-2 h level remained almost unchanged in the affected group, although it was one-half of the fasting level in the control group. Inter-individual analyses revealed that the GSD Ia group mannose level was significantly and positively correlated with lactate and triglycerides levels at both time points ($p<0.01$). In each control, mannose levels fluctuated greatly, maintaining strong and significant negative correlations with glucose and insulin levels ($p<0.001$). Correlations were lower or nonexistent in GSD Ia children. In individuals with high lactate and triglycerides levels, strikingly high mannose levels never changed against glucose and insulin fluctuations. Plasma mannose is less sensitive to blood glucose and insulin in GSD Ia children. Its basal level and the fluctuation pattern differ by their metabolic activity.

Abbreviations

GSD Ia	Glycogen storage disease type Ia
G6Pase	Glucose-6-phosphatase
G6P	Glucose-6-phosphate
AST	Aspartate transaminase
ALT	Alanine transaminase

Introduction

Glycogen storage disease type Ia (GSD Ia), also designated as von Gierke disease (OMIM 232200), is a congenital carbohydrate disorder caused by a deficiency in liver glucose-6-phosphatase (G6Pase), lacking conversion of glucose-6-phosphate (G6P) to glucose in the liver. Aside from profound hypoglycemia attributable to failure of hepatic glucose release to the circulation, diverse metabolic abnormalities such as lactic acidemia, hypertriglyceridemia, and hyperuricemia have been described (Chen 2001; Rake et al 2002). Nevertheless, more information related to the metabolic derangements of GSD Ia is necessary to elucidate the pathophysiology of GSD Ia better and to improve medical intervention.

Mannose is connected to glycogenolysis, which maintains blood glucose concentrations (Fig. 1). This carbohydrate has recently been implicated in promoting cell growth and differentiation, and in inhibiting carcinogenesis and fibrosis of several tissues and organs, including the liver (Kang et al 1999; Ngeow et al 2011; Niehues et al 1998; Oka et al 2002; Prakash et al 2010).

Several reports have described that most plasma mannose is generated from liver glycogen-oriented G6P, and that the mannose concentration is tightly regulated by blood glucose concentration (Taguchi et al 2005; Sone et al 2003) (Fig. 1). Our recent study revealed that patients with glycogen storage disease type 0 (OMIM, 240600), a congenital deficiency in the hepatic isoform of glycogen synthase manifested by decreased liver glycogen, exhibited extremely low plasma mannose levels (Miwa et al 2010). Nevertheless, we have no information related to mannose metabolism in GSD Ia.

This study examined plasma mannose in seven GSD Ia children and compared those concentrations with those of healthy children. We herein describe fasting and postprandial high plasma mannose levels in GSD Ia, which differ greatly from those in healthy children. A possible explanation for such high plasma mannose levels that are less sensitive to blood glucose is discussed.

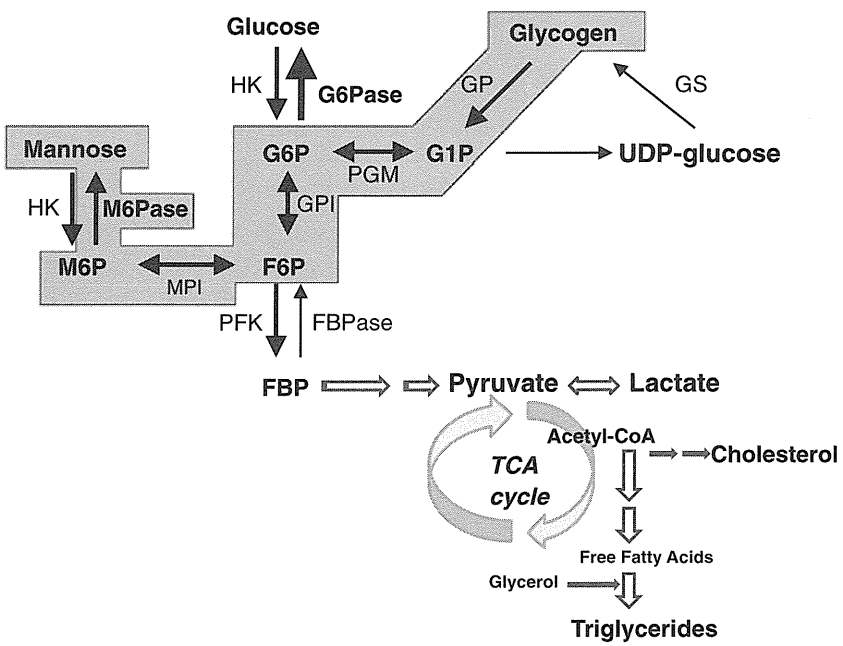

Fig. 1 Hepatic mannose production pathway. Mannose is believed to be derived from glycogen through the pathway indicated by the shaded area. *FBP* fructose 1,6-bisphosphate; *FBPase* fructose-bisphosphatase; *G1P* glucose 1-phosphate; *GP* glycogen phosphorylase; *GPI* glucose-6-phosphate isomerase; *GS* glycogen synthase; *G6Pase* glucose-6-phosphatase; *HK* hexokinase; *MPI* mannose-6-phosphate isomerase; *M6Pase* mannose-6-phosphatase; *PFK* 6-phosphofructokinase; *PGM* phosphoglucomutase

Subjects and methods

Subjects

We enrolled four male and three female GSD Ia children now aged 7–14 years: patients 1–7 (Table 1). Diagnoses were made at the ages of 6 months–1 year 3 months using gene analysis, liver G6Pase activity, together with clinical presentations comprising hepatomegaly (7/7 patients), short stature (1/7; patient 7), and convulsion because of hypoglycemia (4/7; patients 1, 2, 3, and 6). They all showed fasting lactic acidemia (plasma lactate, 4.9–6.4 mmol/L) and mild or moderate elevations of transaminase (AST, aspartate aminotransferase, 62–147 IU/L; ALT, alanine aminotransferase, 62–150 IU/L)

Immediately after the diagnosis, they began to receive frequent meals with galactose-lipid restricted milk and cornstarch to avoid hypoglycemia. All patients were confirmed as homozygous for the G727T mutation, which is highly prevalent in Japanese patients (Chen 2001; Rake et al 2002). Their daily energy intake corresponded to the requirements for their respective ages. The compositions of the diets were the following: carbohydrates, 63–70 %; proteins, 10–17 %; lipids, 15–25 %. Regarding carbohydrates, fructose and galactose were limited to within 5 % of total carbohydrate content (Table 1). To date, they have experienced normal growth and development. At present, their liver transaminase levels are normal or slightly above the respective upper limits. Their livers are still palpable 3–8 cm under the right costal margin. They had never suffered from candidiasis, which possibly increases the plasma mannose level (Manson and Wilkinson 1981).

Study design, sample collection and biochemical assays

After 4.3–5.6 h fasting followed by 1.0–2.0 g/kg of cornstarch intake at 3:00–4:00 AM, we collected blood samples from the six affected children immediately before breakfast (AM 7:00–8:00), supplying one-fourth of their daily energy intake corresponding to their respective requirements, and at 2 h after breakfast (AM 9:00–10:00). The plasma mannose levels were determined together with whole blood glucose, plasma lactate, serum insulin, and serum total cholesterol and triglycerides.

As age-matched healthy controls, we enrolled 6 children: 2 girls and 4 boys aged 10–15 years. Blood samples from them were those immediately before breakfast supplying one-fourth of daily energy intake (AM 7:00–8:00) and 2 h after breakfast (9:00–10:00).

Secondly, for six of the seven patients (patients 1, 2, 3, 5, 6, and 7) and two control children, we examined intra-individual parameter changes that occurred within 1 day by frequent sampling (8–10 points).

This study was approved by the relevant institutional medical ethics review boards. Informed consent was obtained from parents of the enrolled children before this study began.

Biochemical assays

Plasma mannose concentrations were determined using high-performance liquid chromatography, as described in a previous report (Taguchi et al 2005, 2003). Whole blood glucose and plasma lactate levels were determined using enzymatic methods with their respective assay kits (BS Kyowa for glucose and Determiner LA for lactate; Kyowa Medex Co. Ltd., Tokyo, Japan). The serum insulin level was determined using an enzyme immunoassay with a commercial kit (TOSOH-II;

Table 1 Backgrounds of six glycogen storage disease type Ia children

Cases	Ages	Height SD score	BW SD score	Daily energy intake, compositions of nutrients, and cornstarch intakes during last 6 months
1. male	13 y5m	−0.8 SD	+0.2SD	2250–2390 Kcal: carbohydrate 68–70 %, protein 10–15 %, lipids 15–20 % Cornstarch:1.2 g/k,15:00; 1.7 g/k, 22:00/3:00–4:00
2. female	9y11m	−1.3 SD	−0.3SD	2200–2300 Kcal: carbohydrate 70 %, protein 10–14 %, lipids 15–21 % Cornstarch:1.5 g/k, 10:00/15:30;1.8 g/k, 22:00/3:00–4:00
3. male	7y11m	−1.4 SD	−0.4SD	2050–2250 Kcal: carbohydrate 70 %, protein 10–15 %, lipids 15–20 % Cornstarch: 1.4 g/k,10:00/15:00; 1.6 g/k; 22:00/3:00–4:00
4. female	14y6m	−1.2 SD	−0.2SD	2230–2450 Kcal: carbohydrate 70 %, protein 10–15 %, lipids 15–20 % Cornstarch:1.5 g/k, 10:00/15:30;1.5–1.8 g/k, 22:00/3:00–4:00
5. male	14 y2m	−1.8 SD	+0.1SD	2300–2440 Kcal: carbohydrate 63–67 %, protein 12–16 %, lipids 16–21 % Cornstarch:0.5 g/k,15:00;0.5–0.9 g/k; 22:00/3:00–4:00
6. male	12y6m	−1.9 SD	−0.9SD	2250–2350 Kcal: carbohydrate 63–65 %, protein 13–15 %, lipids 18–20 % Cornstarch:1.0 g/k, 10:00/15:30;0.6–1.0 g /k, 22:00/3:00–4:00
7. male	7y11m	−2.0 SD	−0.8SD	2050–2250 Kcal: carbohydrate 63–66 %, protein 13–17 %, lipids 18–22 % Cornstarch: 1.0 g/k,10:00/15:00; 0.5–1 g/k; 22:00/3:00–4:00

BW body weight

* Galactose and fructose were limited within 5 % of carbohydrates

Tosoh Corp., Tokyo, Japan). Serum levels of total cholesterol and triglycerides were determined using enzymatic methods with commercial kits (Kyowa Medex Co. Ltd.). ALT and AST activities in plasma were assayed using commercially available kits.

Statistical analysis

Values between the affected children and control children groups were compared using an unpaired Student *t*-test. Values at two time points within each group were compared using the one-factor ANOVA test. The relation between mannose and other parameters was estimated using the Pearson correlation test. All *p* values less than 0.05 were regarded as significant.

Results

Fasting mannose, lactate, and triglyceride levels in GSD Ia group were significantly higher than those in the control group ($p<0.001$). Total cholesterol concentrations were also increased significantly in GSD Ia group ($p<0.01$). However, the fasting glucose and insulin levels were not different between the GSD Ia and control groups (Table 2).

Inter-individual parameter variations were great among the seven affected children: four affected children (patients 1, 2, 3, and 4) always showed mildly increased fasting lactate and triglyceride levels (lactate<2.5 mmol/L, triglyceride<5.0 mmol/L); three children at suboptimal metabolic control levels (patients 5, 6, and 7) showed moderate or more-increased lactate and triglyceride levels (lactate>3.5 mmol/L, TG>5.5 mmol/L). Therefore, the affected group was divided into two subgroups: subgroup 1, with children having mildly increased parameter levels, and subgroup 2, with children having considerably increased parameter levels. The fasting mannose level in subgroup 2 was significantly higher than that in the subgroup 1($p<0.001$) (Table 2). Carbohydrate intakes of the subgroup 2 children were lower than those of subgroup 1 children (Table 1).

Postprandial-2 h mannose level in the affected group was similar to the fasting level. The value was about four-fold higher than that in the control group. However, the glucose and insulin levels at this time did not differ between these two groups statistically. The lactate level in the affected group was greatly decreased, but it remained significantly higher than that in the control group. In contrast, the triglyceride level was increased substantially in the affected group after a meal. The value was significantly and much higher than the control group's level ($p<0.001$) (Table 2).

The postprandial-2 h mannose level in subgroup 2 was significantly higher than that in subgroup 1 ($p<0.001$). Moreover, lactate and triglyceride levels in subgroup 2 were significantly higher than those in subgroup 1 ($p<0.001$) (Table 2). The decrease in the postprandial-2 h mannose level was statistically significant, but mild ($p<0.05$) in subgroup 1, although it was not significant in group 2. Postprandial-2 h mannose levels in the controls were decreased significantly ($p<0.001$) to one-half of the fasting level (Table 2).

Among the six children belonging to the control group, the fasting and postprandial-2 h mannose levels showed significant correlations with the respective insulin and glucose levels: glucose, $p<0.01$ at the fasting point and $p<0.05$ at

Table 2 Fasting- and postprandial-2 h levels of carbohydrates and lipids in GSD Ia and control children

	Mannose (μmol/l)	Glucose (mmol/l)	Lactate (mmol/l)	Insulin (μU/ml)	Triglycerides (mmol/L)	T-cholesterol (mmol/L)
# GSD Ia group (n=7)						
fasting (n=7)	55±11***	4.7±0.2	2.8±0.9***	7.1±0.3	4.2±0.5***	5.7±0.4**
post-2 h (n=7)	51±10***	6.7±0.2	1.4±0.2***	47.5±2.1	5.6±0.8***	6.1±0.6**
subgroup 1 fasting (n=4)	45±8***	4.9±0.3	1.9±0.2***	7.2±0.3	3.7±0.7***	5.1±0.6*
subgroup 1 post-2 h (n=4)	35±7***	6.1±0.2	1.1±0.2	45.5±3.4	4.2±1.1***	5.5±0.6*
subgroup 2 fasting (n=3)	71±12***	4.6±0.3	3.8±0.4***	7.0±0.4	6.9±1.0***	6.3±0.8***
subgroup 2 post-2 h (n=3)	73±14***	5.9±0.2	1.6±0.3**	41.4±3.5	7.6±1.4***	6.6±0.5***
Control group (n=6)						
fasting (n=6)	30±4	4.6±0.2	0.8±0.1	7.5±0.5	0.7±0.1	4.5±0.2
post-2 h (n=6)	16±3	6.4±0.1	0.9±0.1	44.3±3.5	1.1±0.1	4.6±0.2

Values of children are presented as means ± SD

GSD children were divided into two subgroups according to the metabolic controls: subgroup 1; four fairly-controlled patients taking mostly appropriate calory and nutrients; subgroup 2, three unsatisfactorily controlled patients taking insufficient carbohydrates and cornstarch

Fasting and postprandial samples were collected before breakfast and 2 h after breakfast, respectively

* $p<0.05$, ** $p<0.01$, *** $p<0.001$ vs. controls

Table 3 Correlations of mannose with other metabolic parameters in the affected (n=7) and control (n=6) groups

		Glucose	Lactate	Insulin	Triglycerides	T-cholesterol
Fasting	Affected group	0.376	0.945**	0.372	0.888**	0.649*
	Control group	−0.895**	0.221	−0.811*	−0.172	0.312
Post-2 h	Affected group	−0.260	0.983**	0.423	0.956**	0.679*
	Control group	−0.818*	0.165	−0.934**	0.169	0.277

Presented data were r-values

* $p<0.05$, ** $p<0.01$

postprandial-2 h; insulin, $p<0.05$ at the fasting point and $p<0.01$ at postprandial-2 h (Table 3). Among the seven children of the affected group, the fasting and postprandial-2 h mannose levels showed significant correlations with the respective lactate, triglycerides, and total cholesterol levels (lactate and triglycerides, $p<0.01$; total cholesterol, $p<0.05$) but not with the respective insulin and glucose levels (Table 3).

One-day monitoring of intra-individual parameter changes revealed strong negative correlation of plasma mannose level with glucose and insulin levels in the two control children ($p<0.001$) (Table 4). Such correlations were not detected in patients 5, 6, and 7 belonging to subgroup 2, although they were significant but only mild ($p<0.05$) in patients 1, 2, and 3 belonging to subgroup 1 (Table 4).

Discussion

Results of this study demonstrate clearly that the plasma mannose concentrations in children with GSD Ia are much higher than that in healthy control children. Unlike the control children, the postprandial decrease in the plasma mannose level was obscure in the affected children, i.e., their plasma mannose levels remained high, being less sensitive to diet and blood glucose level. Such a carbohydrate abnormality has not been described in GSD Ia.

Table 4 Correlations between mannose and other parameters in six affected and two control children by one-day intra-individual successive examination

	Glucose	Lactate	Insulin	Triglycerides	T-cholestrol
Patient 1	−0.599*	0.555	−0.695*	−0.567*	−0.318
Patient 2	−0.656*	0.629*	−0.666*	−0.655*	−0.492
Patient 3	−0.597*	0.618*	−0.602*	−0.615*	−0.228
Patient 5	−0.244	0.198	−0.258	−0.119	−0.253
Patient 6	−0.235	0.211	−0.009	−0.298	−0.366
Patient 7	0.069	0.154	0.111	−0.101	−0.193
Control 1	−0.965***	−0.123	−0.985***	−0.368	0.007
Control 2	−0.976***	0.226	−0.979***	−0.295	−0.114

For six of seven patients and two of six controls, blood parameters were repeatedly determined at various time points (ten times), including fasting times and postprandial times

Presented data were r-values

* $p<0.05$, ** $p<0.01$, *** $p<0.001$

Our previous studies provided evidence that most plasma mannose is supplied from liver glycogen via the following pathway: glycogen→glucose 1-phosphate→glucose 6-phosphate→fructose 6-phosphate→mannose 6-phosphate→mannose (Fig. 1) (Taguchi et al 2005, 2003; Sone et al 2003; Pederson et al 1998). These results also demonstrated that postprandial plasma mannose levels are much lower than those in the fasting condition (Taguchi et al 2005; Sone et al 2003). The fasting and postprandial mannose levels in the control children were consistent with such results. Postprandial decreases of the plasma mannose level have been inferred as a result of the suppression of hepatic glycogenolysis attributable to the increase of the plasma insulin level, in concert with an elevation of blood glucose level (Taguchi et al 2005; Sone et al 2003). Actually, in our control children, plasma mannose levels were reciprocally and greatly decreased continuously with the increased insulin level or glucose level, supporting an inhibitory effect of insulin or glucose on mannose generation.

Earlier reports have described that mannose production is increased and less sensitive to blood glucose in patients with

Table 5 Mannose concentrations in children with GSD type III, IX and Ib

Patients	Type		Mannose (μmol/l)	Glucose (mmol/l)	Insulin (μU/ml)
1. 7-year-boy	GSD IX	fasting	29	4.5	7.1
		post-2 h	21	6.8	47.5
2. 8-year-boy	GSD IX	fasting	28	4.6	7.5
		post-2 h	16	6.1	43.8
3. 7-year-girl	GSD III	fasting	24	4.4	6.2
		post-2 h	12	6.6	49.5
4. 10-year-boy	GSD III	fasting	24	4.6	7.3
		post-2 h	14	6.2	51.4
5. 14-year-boy	GSD Ib	fasting	70	4.8	9.2
		post-2 h	68	7.0	52.3

GSD IX, glycogen phosphorylase kinase b deficiency; GSD III, debrancing enzyme deficiency:

GSD Ib glucose-6-transport deficiency

GSD IX and III were diagnosed at 6 months-2 years by enzyme activity and gene analyses

GSD Ib was diagnosed at 10 months by the clinical manifestation and gene analyses

All children have received dietary therapies using cornstarch to avoid hypoglycemia after the diagnosis

diabetes mellitus, in particular poorly controlled subjects accompanying hyperlipidemia and fatty liver (Sone et al 2003). We will therefore investigate the mannose metabolism in terms of hepatic insulin resistance—a liver condition that is often found in fatty liver and which presents unregulated glycogenolysis (Yadav et al 2009; Konopelska et al 2011).

Mannose levels in affected children having high basal lactate and triglycerides levels were strikingly increased and were entirely independent of the glucose and insulin levels, although those in patients having almost normal basal lactate levels, together with moderately increased triglycerides level, showed significant but only weak correlations. Inter-individual correlation analyses for the affected group revealed significant positive correlations of plasma mannose with plasma lactate and serum triglycerides both at a fasting time and postprandial-2 h. Such positive correlations were also found in each by intra-individual successive parameter pursuits.

Kuipers and his colleagues reported that de novo synthesis of triglycerides and cholesterol were increased intensively in GSD Ia. They contributed greatly to the remarkable hypertriglyceridemia (Bandsma et al 2008; Wang et al 2011). Accumulated G6P in the liver is expected to be directed easily toward lactate production and Krebs cycle generating acetyl-CoA, a substrate for free fatty acids and triglycerides (Fig. 1). From this context, we inferred that high fasting- and postprandial-2 h mannose levels in the affected children reflected the high content of G6P in the liver as a consequence of the low or absent activity of liver G6Pase. Therefore, the mannose level is expected to be linked more closely to lactate and triglyceride levels in GSD children than in healthy children.

We reported previously that children with glycogen storage disease type 0 presenting poor liver glycogen exhibited extremely low plasma mannose levels (Miwa et al 2010). Recently, we examined mannose levels in five preadolescent or adolescent patients with liver GSD of other types: two patients with liver phosphorylase kinase b deficiency, GSD type IX, (OMIM 300798); two patients with debranching enzyme deficiency, GSD type III, (OMIM 300798); and one patient with glucose-6-transport defect, GSD type Ib (OMIM 602671) (Table 5). Their diagnoses were confirmed using gene analyses, clinical presentations and liver enzyme activities. After the diagnoses, they all received diet therapies using cornstarch to avoid hypoglycemia. In patients with GSD type IX and III, liver-glycogen oriented G6P is not increased theoretically (Chen 2001; Davit-Spraul et al 2011; Davit-Spraul 2007; Heller et al 2008). Their mannose levels were similar to the controls' levels and were sensitive to the blood glucose and insulin as the control children (Table 5). However, the mannose level in a patient with GSD type Ib was similar to patients with GSD Ia. These data suggest that liver-oriented G6P is a determinant for plasma mannose, and that elevated mannose concentrations are specific for the GSD I subtype, i.e., GSD Ia and GSD Ib.

Results show that mannose fluctuates according to the metabolic control of GSD Ia. Earlier reports have described that metabolic control is closely related to the development of hepatocellular adenoma in long-standing GSD Ia (Wang et al 2011; Parker et al 1993). However, the pathogenesis of adenoma development remains unknown. Aside from mannose, many carbohydrates and lipids often exhibit prominent increases in GSD Ia when the metabolic control is poor. Whether an increased mannose content, possibly in association with other metabolic anomalies, is involved in the pathogenesis of hepatic adenoma in GSD Ia remains speculative and should be investigated in future studies. According to earlier reports, it is plausible that mannose acts against transforming growth factor-β -induced liver fibrosis, and supports an inhibitory effect of mannose-6-phosphate/insulin-like growth factor II receptor on liver carcinogenesis (Kang et al 1999; Ngeow et al 2011; Niehues et al 1998; Oka et al 2002; Prakash et al 2010).

In conclusion, results of this study suggest that alterations in G6P metabolism influence mannose production, and that mannose is an excellent biomarker for GSD I.

Conflict of interest None.

References

Bandsma RH, Princen BH, van der Velden MD et al (2008) Increased de novo lipogenesis and delayed conversion of large VLDL into IDL particles contribute to hyperlipidemia in Glycogen storage disease type Ia. Pediatr Res 63:72–77

Chen Y-T (2001) Glycogen storage diseases. In: Scriver CR, Beaudet AL, Sly WS, Valle D (eds) The metabolic and molecular bases of inherited disease, Eighthth edn. McGraw-Hill, New York, pp 1521–1551

Davit-Spraul A (2007) Glycogen storage diseases: new perspectives. World J Gastroenterol 13:2541–2553

Davit-Spraul A, Piraud M, Dobbelaere D et al (2011) Liver glycogen storage diseases due to phosphorylase system deficiencies: diagnosis thanks to non invasive blood enzymatic and molecular studies. Mol Genet Metab 104:137–143

Heller S, Worona L, Consuelo A (2008) Nutritional therapy for glycogen storage diseases. J Pediatr Gastroenterol Nutr 47:S15–S21

Kang JX, Bell J, Beard RL, Chandraratna RA (1999) Mannose 6-phosphate/insulin-like growth factor II receptor mediates the growth-inhibitory effects of retinoids. Cell Growth Differ 10:591–600

Konopelska S, Kienitz T, Quinkler M (2011) Down-regulation of hepatic Glucose-6-Phosphatase-α in patients with hepatic steatosis. Obesity (Silver Spring) 19:2322–2326

Manson TP, Wilkinson KP (1981) Mannose in body fluids as an indicator of invasive candidiasis. J Clin Microbiol 14:557–562

Miwa I, Taguchi T, Asano H et al (2010) Low level of fasting plasma mannose in a child with glycogen storage disease type 0 (liver glycogen synthase deficiency). Clin Chim Acta 411:998–999

Ngeow WC, Atkins S, Morgan CR, Metcalfe AD et al (2011) The effect of Mannose-6-Phosphate on recovery after sciatic nerve repair. Brain Res 1394:40–48

Niehues R, Hasilik M, Alton G et al (1998) Carbohydrate-deficient glycoprotein syndrome type Ib. Phosphomannose isomerase deficiency and mannose therapy. J Clin Invest 101:1414–1420

Oka Y, Waterland RA, Killian JK et al (2002) M6P/IGF2R tumor suppressor gene mutated in hepatocellular carcinomas in Japan. Hepatology 35:1153–1163

Parker PH, Ballew M, Greene HL (1993) Nutritional management of glycogen storage disease. Annu Rev Nutr 13:83–109

Pederson BA, Foster ID, Nordlie RC (1998) Low-Km mannose-6-phosphatase as a criterion for microsomal integrity. Biochem Cell Biol 76:15–24

Prakash J, Beljaars L, Harapanahalli AK et al (2010) Tumor-targeted intracellular delivery of anticancer drugs through the mannose-6-phosphate/insulin-like growth factor II receptor. Int J Cancer 126:1966–1981

Rake JP, Visser G, Labrune P et al (2002) Glycogen storage disease type I: diagnosis, management, clinical course and outcome. Results of the European study of glycogen storage disease type I (ESGSD I). Eur J Pediatr 161(Suppl 1):S20–S34

Sone H, Shimano H, Ebinuma H et al (2003) Physiological changes in circulating mannose levels in normal, glucose-intolerant, and diabetic subjects. Metabolism 52:1019–1027

Taguchi T, Miwa I, Mizutani T et al (2003) Determination of D-mannose in plasma by HPLC. Clin Chem 49:181–183

Taguchi T, Yamashita E, Mizutani T et al (2005) Hepatic glycogen breakdown is implicated in the maintenance of plasma mannose concentration. Am J Physiol Endocrinol Metab 288:E534–E540

Wang DQ, Fiske LM, Carreras CT et al (2011) Natural history of hepatocellular adenoma formation in glycogen storage disease type I. J Pediatr 159:442–446

Yadav H, Jain S, Yadav M et al (2009) Epigenomic derangement of hepatic glucose metabolism by feeding of high fructose diet and its prevention by Rosiglitazone in rats. Dig Liver Dis 41:500–508

J Inherit Metab Dis
DOI 10.1007/s10545-012-9526-6

ORIGINAL ARTICLE

Two neonatal cholestasis patients with mutations in the *SRD5B1* (*AKR1D1*) gene: diagnosis and bile acid profiles during chenodeoxycholic acid treatment

Yoshitaka Seki · Tatsuki Mizuochi · Akihiko Kimura · Tomoyuki Takahashi · Akira Ohtake · Shin-Ichi Hayashi · Toshiya Morimura · Yasuharu Ohno · Takayuki Hoshina · Kenji Ihara · Hajime Takei · Hiroshi Nittono · Takao Kurosawa · Keiko Homma · Tomonobu Hasegawa · Toyojiro Matsuishi

Received: 19 October 2011 / Revised: 19 July 2012 / Accepted: 25 July 2012

Abstract
Background and aims In two Japanese infants with neonatal cholestasis, 3-oxo-Δ^4-steroid 5β-reductase deficiency was diagnosed based on mutations of the *SRD5B1* gene. Unusual bile acids such as elevated 3-oxo-Δ^4 bile acids were detected in their serum and urine by gas chromatography–mass spectrometry. We studied effects of oral chenodeoxycholic acid treatment.
Patients and methods *SRD5B1* gene analysis used peripheral lymphocyte genomic DNA. Diagnosis and treatment of these two patients were investigated retrospectively and prospectively investigated.
Results With respect to *SRD5B1*, one patient was heterozygous (R266Q, a novel mutation) while the other was a compound heterozygote (G223E/R261C). Chenodeoxycholic acid treatment was effective in improving liver function and decreasing unusual bile acids such as 7α-hydroxy- and 7α,12α-dihydroxy-3-oxo-4-cholen-24-oic acids in serum and urine.

Communicated by: Peter Theodore Clayton

Y. Seki · T. Mizuochi · A. Kimura (✉) · T. Takahashi · T. Matsuishi
Department of Pediatrics and Child Health,
Kurume University School of Medicine,
67 Asahi-machi,
Kurume-shi 830-0011, Japan
e-mail: hirof@med.kurume-u.ac.jp

T. Takahashi
Division of Gene Therapy and Regenerative Medicine,
Cognitive and Molecular Research Institute of Brain Disease,
Kurume University,
Kurume, Japan

A. Ohtake
Department of Pediatrics, Faculty of Medicine,
Saitama Medical University,
Saitama, Japan

S.-I. Hayashi · T. Morimura · Y. Ohno
Department of Pediatric Surgery, Faculty of Medicine,
Saitama Medical University,
Saitama, Japan

T. Hoshina · K. Ihara
Department of Pediatrics, Graduate School of Medical Sciences,
Kyushu University,
Fukuoka, Japan

H. Takei · H. Nittono
Institution of Bile Acid, Junshin Clinic,
Tokyo, Japan

T. Kurosawa
Faculty of Pharmaceutical Sciences,
Health Sciences University of Hokkaido,
Hokkaido, Japan

K. Homma
Central clinical Laboratories, Keio University Hospital,
Tokyo, Japan

T. Hasegawa
Department of Pediatrics, Keio University School of Medicine,
Tokyo, Japan

Published online: 16 November 2012